A Gradient-Based Inverse Lithography Technology for Double-Dipole Lithography

Wei Xiong, Jinyu Zhang, Yan Wang, and Zhiping Yu
Institute of Microelectronics
Tsinghua University
Beijing, China, 100084
E-mail address: xiongwei00@mails.tsinghua.edu.cn

Min-Chun Tsai
Brion Technologies, Inc.
An ASML company
Santa Clara, CA 95054, USA
E-mail address: mitsai@brion.com

***Abstract*—Resolution enhancement techniques (RETs) have become indispensable for the sub-wavelength optical lithography. Inverse lithography technology (ILT) is one kind of RETs, which attempts to consider the mask synthesis as an inverse problem and compute the optimum mask by using the entire area of the design pattern with a rigorous mathematical approach. Double-dipole lithography (DDL) uses two orthogonal dipole illuminations and one or two masks to print the desired wafer pattern. The main challenge of using such an IC-manufacturing technique remains how to properly synthesize the proper mask pattern for the arbitrarily given target pattern. This paper presents a gradient-based ILT approach addressing the problem above, called DDL-ILT. This method has been demonstrated by synthesizing various kinds of masks for printing 45-nm critical dimension (CD) features. Images with good fidelity have been achieved.**

Keywords-ILT; mask synthesis; double-dipole lithography; gradient-based; phase-shifting masks

I. INTRODUCTION

Resolution Enhancement Techniques (RETs) are widely used to cope with the severe optical distortions in sub-wavelength lithography. Inverse lithography technology (ILT) has been proposed as an option for RETs. The pioneer work in ILT was by Saleh and Sayegh [1]. Recently, there have been a number of research concerns in ILT approaches [2-5]. Erdmann [2] proposed genetic algorithms (GA) to synthesize the masks. Granik [3] used nonlinear programming to solve the inverse problem. Poonawala and Milanfar [4] developed a gradient-based method to perform optimization. However, their method only focused on incoherent and coherent imaging systems. Davids and Bollepalli [5] have described ILT suitable to partially-coherent imaging system.

Double-dipole lithography (DDL) [6][7] refers to a novel double-exposure technique that uses one or two masks, in which each is correspondingly exposed with optimized dipole illumination for realizing sub-wavelength optical lithography. Dipole illumination is the most extreme case of off-axis illumination (OAI). It is capable of providing better imaging contrast with improved process window. The limitation of using dipole illumination lies in that it only enhances the resolution for features orthogonal to the illumination pole axis. In [6] and [7], authors decompose the mask pattern into two parts by using the horizontal and vertical decomposition. The horizontal features of the mask pattern are printed during the first exposure while using a vertical-dipole illumination. The illumination above suppresses the features along the vertical direction. The second exposure uses a horizontal-dipole illumination and accounts for the vertical features. The decomposition above needs to be performed along with model-based OPC to guarantee that the corners and junctions are accurately reproduced. However, recent studies have shown that the edge-based approaches [8] such as OPC methods may not be very suitable for 45-nm and smaller nodes due to the increase in the fragmentation and inability to generate assist bars, etc.

Poonawala and Milanfar [9] combined the two techniques: double-exposure lithography and inverse lithography, and proposed a double-exposure inverse lithography (DEL-ILT) framework. They tested chromeless phase-shifting masks (CPSM) for an idealized case of a coherent imaging system. However, it is more complicated and more expensive to manufacture CPSM compared to the production of binary masks. In addition, it is highly desirable to use the partially coherent imaging model instead of the coherent imaging model for improving the accuracy.

In this work, we construct a novel ILT-based framework combined with DDL (DDL-ILT) for 45-nm mask synthesis. This proposed framework uses the partially coherent imaging model, and can be used for designing various kinds of masks such as binary masks and CPSM. Since this framework combines ILT and DDL, it remarkably enhances the imaging resolution in optical lithography. This approach has been demonstrated using different mask technologies. Good fidelity images have been achieved when CD is reduced to 45-nm with 15×15 nm^2 pixel size.

II. IMAGING MODEL IMPLEMENTATION

A. *Partially Coherent Imaging Model for Single-Exposure Lithography (SEL) Systems*

Hopkins' Equation [10] and the Sum-of-Coherent-System (SOCS) theory [11] are widely used for modeling the partially coherent lithography systems and the aerial image intensity distribution can be calculated as

$$i(x,y)=\sum_{l=1}^{P}\sigma_l\left|(\phi_l\otimes m)(x,y)\right|^2, \quad (1)$$

where $\phi_1,\phi_2,\ldots,\phi_P$ are the kernels of the partially coherent lithography system and $\sigma_1,\sigma_2,\ldots,\sigma_P$ are the corresponding weighted coefficient; the coefficients quickly decay to zero, thereby facilitating an accurate approximation with the P-th order; $m(x,y)$ is the mask transmission function; the notation $\otimes$ represents the convolution operator.

The constant threshold resist (CTR) model [4] is used to model the resist action when calculating the final wafer image. It is described using a step function as

$$\Gamma(v)=\begin{cases}0, & v\le t_{\mathrm{r}}\\ 1, & v>t_{\mathrm{r}}\end{cases}, \quad (2)$$

where t_{r} is the threshold of the resist. Thus the wafer image can be computed as

$$Z(x,y)=\Gamma\Big(\sum_{l=1}^{P}\sigma_l\left|(\phi_l\otimes m)(x,y)\right|^2\Big). \quad (3)$$

Equation (3) is used to model the partially coherent imaging system with single exposure in this work.

B. Formulation of DDL

The illumination scheme has an important effect on the resolution of the optical lithography system. Fig. 1 illustrates two illumination schemes: annular illumination and dipole illumination. The annular illumination scheme has two parameters: the inner coherence $\sigma_{\mathrm{in\_ann}}$ and the outer coherence $\sigma_{\mathrm{out\_ann}}$. The dipole illumination scheme has three parameters: the inner coherence $\sigma_{\mathrm{in\_dip}}$, the outer coherence $\sigma_{\mathrm{out\_dip}}$ and the pole direction (horizontal or vertical).

The annular illumination is applicable to SEL system because the dipole illumination has a limitation that it only enhances resolution for features that are orthogonal to the illumination pole axis. Thus, the dipole illumination is usually used for DDL systems. In this work, we consider DDL systems where only one mask is exposed by the two exposures and the resist is developed only once at the end of the two exposures. The final aerial image for the given DDL system is equal to the sum of the aerial images obtained from the two individual exposures. Similar to SEL systems, the aerial image $i_{\mathrm{DDL}}(x,y)$ and the wafer image $Z_{\mathrm{DDL}}(x,y)$ can be modeled as

$$i_{\mathrm{DDL}}(x,y)=\sum_{l=1}^{P_1}\gamma_l\left|(\xi_l\otimes m_{\mathrm{DDL}})(x,y)\right|^2+\sum_{l=1}^{P_2}\tau_l\left|(\eta_l\otimes m_{\mathrm{DDL}})(x,y)\right|^2$$

$$Z_{\mathrm{DDL}}(x,y)=\Gamma(i_{\mathrm{DDL}}(x,y)), \quad (4)$$

where $\xi_1,\ldots,\xi_{P_1}$ and $\eta_1,\ldots,\eta_{P_2}$ are the kernels corresponding to the two dipole illuminations, respectively; $\gamma_1,\ldots,\gamma_{P_1}$ and $\tau_1,\ldots,\tau_{P_2}$ respectively correspond to their singular values; $m_{\mathrm{DDL}}(x,y)$ is the mask transmission function in DDL.

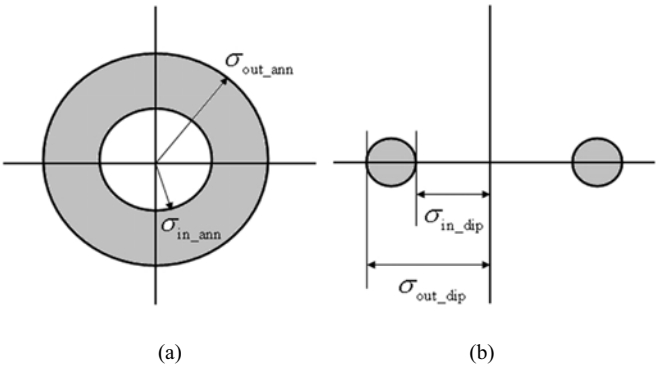

Figure 1. Examples of two illumination schemes: (a) annular illumination; (b) dipole illumination.

III. Mask-synthesis Problem Formulation

The most important step of DDL-ILT approach is how to find the optimal mask. This problem is described in details in this section.

A. Parameters Definition and Transformation

The practical mask transmission is not continuous, since it is constrained by the type of chosen masks. For example, the transmission values take 0 or 1 for binary masks and take -1 or 1 for CPSM. However, we can reduce this discrete constrained optimization problem to a continuous unconstrained one by using specific parametric transformations. Take binary masks for instance, we can calculate the wafer image as [4]

$$\mathbf{Z}=\mathrm{sig}\left(\sum_{l=1}^{P_1}\gamma_l\left|\mathbf{H}_l\otimes\mathbf{m}\right|^2+\sum_{l=1}^{P_2}\tau_l\left|\mathbf{G}_l\otimes\mathbf{m}\right|^2\right)$$
$$\mathbf{m}=0.5\cdot(1+\cos(\boldsymbol{\theta})) \quad (5)$$

where $\mathbf{m},\mathbf{Z}\in\mathbb{R}^{N_1\times N_2}$ are the matrix representations of m_{DDL} and Z_{DDL}, respectively; (N_1 and N_2 correspond to the numbers of pixels along the horizontal and vertical directions.) $\mathbf{H}_l$ and $\mathbf{G}_l$ are respectively the matrix representations of ξ_l and η_l; $\boldsymbol{\theta}\in\mathbb{R}^{N_1\times N_2}$ is the transformed parameter matrix which is continuous and unconstrained. The logarithmic sigmoid function $\mathrm{sig}(\cdot)$ is used to substitute the step function in (2),

$$\mathrm{sig}(v)=\left[1+\exp(-a(v-t_r))\right]^{-1}, \quad (6)$$

where a indicates the steepness of the sigmoid and the resist threshold t_{r} is the same as that in (2).

Assuming $\mathbf{Z}^{\triangle}$ as the desired pattern (in matrix representation), if we define the cost function $F(\cdot)$ as the L_2 norm of difference between $\mathbf{Z}^{\triangle}$ and $\mathbf{Z}$, the mask-synthesis problem then can be converted into finding the optimal parameter $\boldsymbol{\theta}_{\mathrm{opt}}$ which minimizes the cost function, namely

$$\boldsymbol{\theta}_{\mathrm{opt}}=\arg\min_{\boldsymbol{\theta}}[F(\boldsymbol{\theta})]=\arg\min_{\boldsymbol{\theta}}\left\|\mathbf{Z}-\mathbf{Z}^{\triangle}\right\|_2^2. \quad (7)$$

Now the mask-synthesis problem becomes a continuous and unconstrained optimization problem.

B. Gradient-Based Optimization Scheme

The mask-synthesis problem formulated by (7) can be solved by using the gradient-based optimization scheme because it is continuous and unconstrained. We can analytically calculate the first-order derivatives of $F(\boldsymbol{\theta})$ in (7) using the following expression,

$$\nabla F(\boldsymbol{\theta}) = 2a \cdot \sin(\boldsymbol{\theta}) \cdot \mathrm{Re}\left(\begin{array}{l} \sum_{l=1}^{P_1} \left(\gamma_l \cdot (\mathbf{H}_l^{\circ})^{*} \otimes [\mathbf{X}(\boldsymbol{\theta}) \odot (\mathbf{H}_l \otimes \frac{1+\cos(\boldsymbol{\theta})}{2})] \right) \\ + \sum_{l=1}^{P_2} \left(\tau_l \cdot (\mathbf{G}_l^{\circ})^{*} \otimes [\mathbf{X}(\boldsymbol{\theta}) \odot (\mathbf{G}_l \otimes \frac{1+\cos(\boldsymbol{\theta})}{2})] \right) \end{array} \right), \quad (8)$$

where $\mathbf{X}(\boldsymbol{\theta}) = (\mathbf{Z}^{\Delta} - \mathbf{Z}(\boldsymbol{\theta})) \odot \mathbf{Z}(\boldsymbol{\theta}) \odot (1 - \mathbf{Z}(\boldsymbol{\theta}))$ and notation $\odot$ is the Hadamard product (element-by-element multiplication) of the two matrices; $\mathbf{H}_l^{\circ}$ and $\mathbf{G}_l^{\circ}$ respectively rotates matrices $\mathbf{H}_l$ and $\mathbf{G}_l$ by 180° ; notation * means complex conjugate.

Equation (8) is the foundation to apply gradient-based algorithm in ILT optimization. Poonawala [9] proposed similar results for the coherent double-exposure imaging systems. Note that the coherent imaging is only used for academic study for it lowers the resolution of the optical imaging system and limits the mask types available for inverse imaging.

Then we can use the steepest descent iterations to calculate the optimal mask as

$$\boldsymbol{\theta}^{(k+1)} = \boldsymbol{\theta}^{(k)} - d \cdot \nabla F(\boldsymbol{\theta}^{(k)}), \quad (9)$$

where d is the step size.

C. Penalty Function

The inverse lithography problem is an ill-posed problem. It means that there may be many discrete-tone masks all capable of providing good contour fidelity for a given pattern. In fact, continuous tone masks obtained by using (7) are not physically realizable and we are only interested in solutions comprising of two or three tones. Introducing the penalty functions [4] will help us find the preferred solution.

For binary masks, the penalty function can be chosen as

$$R(\boldsymbol{\theta}) = \left\| \sin^2(\boldsymbol{\theta}) \right\|_1. \quad (10)$$

Thus the mask-synthesis problem formulation is described as

$$\boldsymbol{\theta}_{\mathrm{opt}} = \arg\min_{\boldsymbol{\theta}} [\lambda_{\mathrm{fid}} F(\boldsymbol{\theta}) + \lambda_{\mathrm{pen}} R(\boldsymbol{\theta})], \quad (11)$$

where λ_{fid} and λ_{pen} are the optimization weights. With the penalty function, we favor the estimated pixels to have values closer to 0 and 1 while exploiting the search space. Even so, we need a post-proceeding operation to find the optimal threshold t_{opt} to convert $\boldsymbol{\theta}_{\mathrm{opt}}$ into a physically realizable mask pattern $\boldsymbol{\theta}_{\mathrm{opt}}^{\Delta}$. For example, we can simply obtain the synthesized binary mask pattern $\boldsymbol{\theta}_{\mathrm{opt}}^{\Delta}$ by setting t_{opt} to 0.5.

IV. Simulation Results

In this section, our DDL-ILT approach is validated by applying it to mask synthesis for DDL system. The parameters of DDL systems are set as follows: the wavelength is 193 nm, 0.8 for the numerical aperture and 0.247 for the resist threshold; the dipole illumination has an inner coherence of up to 0.65 and an outer coherence of up to 0.95; 15×15 nm^2 pixel size is used for CD = 45 nm and the target patterns all have 48 pixels in horizontal and vertical direction.

Fig. 2 shows the desired patterns which include "wing", "double snake" and "door" and the X-Y labels are pixel numbers. These patterns are typical layouts of Metal 1 (M1) where the hot-spots often happen. They are also considered as the original binary mask patterns without being synthesized. The black pixels represent the opaque area with a transmission value of 0, while the white pixels represent the transparent area with a transmission value of 1. If we directly use these original masks to obtain the desired pattern, we will get "nothing" on the wafer due to the serious optical proximity effects (OPE). DDL-ILT approach can be used to solve this problem and the simulation results are presented below.

We can apply DDL-ILT approach to the original mask shown in Fig. 2(a), namely "wing". The synthesized mask pattern is shown in Fig. 3(a). And Fig. 3(b) illustrates the corresponding output wafer image pattern. The black bold lines indicate the contour of the desired pattern, while the gray area is the wafer image after exposure and development. The pattern distortion error (PDE) of the wafer image has been reduced from 144 to 20.39. PDE is the total area of where the output wafer image does not match the desired pattern. (The unit of measure is the area of a unit pixel.) The results were obtained from 300 iterations and the run-time was 324s. (all run-times reported were calculated on a 1.66G-Hz Pentium-M based platform using Matlab.)

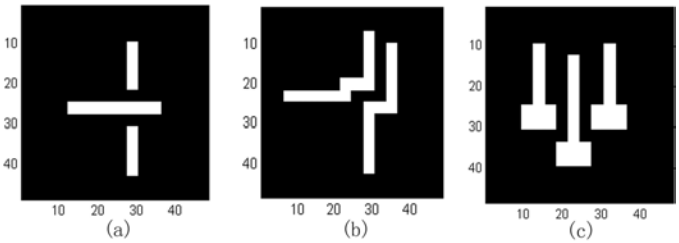

Figure 2. The desired wafer patterns i.e. the original binary mask patterns: (a) "wing"; (b) "double snake"; (c) "door".

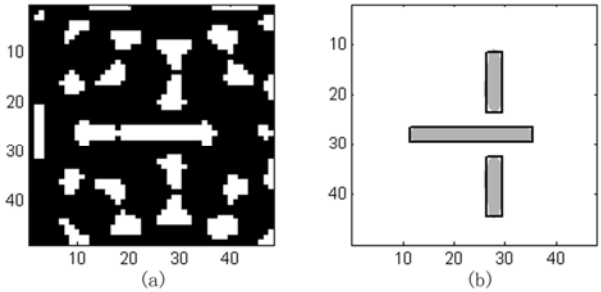

Figure 3. The simulation results for synthesizing binary mask: (a) the synthesized binary mask where black and white pixels have values of 0, 1 respectively; (b) the corresponding image on wafer.

For 6% EPSM, every pixel can only have two transmission values of -0.245 (the 180° phase shift with weak transmission) or 1 (100% transmission with no phase shift). Similar to the binary mask, the following parametric transformation is used,

$$\mathbf{m} = 0.6225 \cdot (1 + \cos(\boldsymbol{\theta})) - 0.245 . \quad (12)$$

And the following specific penalty function is employed, where pixels having values -0.245 and 1 have zero penalty and the cost increases as we move towards the center of the range,

$$R(\boldsymbol{\theta}) = 0.3875 \cdot \left\| \sin^2(\boldsymbol{\theta}) \right\|_1 . \quad (13)$$

Considering the "double snake" pattern in Fig. 2(b), we can obtain the synthesized 6% EPSM illustrated in Fig. 4(a). The white and black regions represent the transmission values of 1 and -0.245, respectively. Fig. 4(b) indicates that the image fidelity is greatly improved when we use the synthesized 6% EPSM to produce the wafer image, compared to directly using the original mask to obtain the wafer pattern. The PDE reduces to 40.08 after mask synthesis. (The initial PDE before mask synthesis is 251.) It took 500 iterations and 521s to obtain the results above.

The final type of masks to be synthesized is APSM. For APSM, the pixels can have values of 0 (opaque) or 1 (100% transmission with no phase shift) or -1 (100% transmission with 180° phase shift). The parametric transformation and penalty function are employed as

$$\mathbf{m} = \cos(\boldsymbol{\theta}) , \quad (14)$$

$$\begin{aligned} R(\boldsymbol{\theta}) = \| & \sin(1.341 \cdot \cos(\boldsymbol{\theta}) + 1.571) \\ & + 0.1975 \cdot \sin(5.71 \cdot \cos(\boldsymbol{\theta}) - 1.571) \\ & + 0.06352 \cdot \sin(12.09 \cdot \cos(\boldsymbol{\theta}) - 1.571) \|_1 \end{aligned} . \quad (15)$$

The penalty function in (15) has maxima at $\cos(\boldsymbol{\theta}) = -0.33$ and 0.33, and minima at $\cos(\boldsymbol{\theta}) = -1$, 0 and 1.

Fig. 5(a) illustrates the synthesized APSM for the "door" pattern shown in Fig. 2(c). The black, gray and white regions respectively correspond to -1, 0 and 1. Fig. 5(b) indicates that nice fidelity of final wafer image has been achieved. The PDE has been reduced from 315 to 37.78 and the simulation process took 500 iterations and 524s.

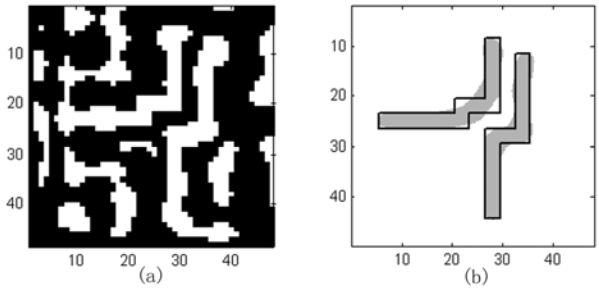

Figure 4. The simulation results for synthesizing 6% EPSM: (a) the synthesized 6% EPSM mask where black and white pixels have values of -0.245, 1 respectively; (b) the corresponding image on wafer.

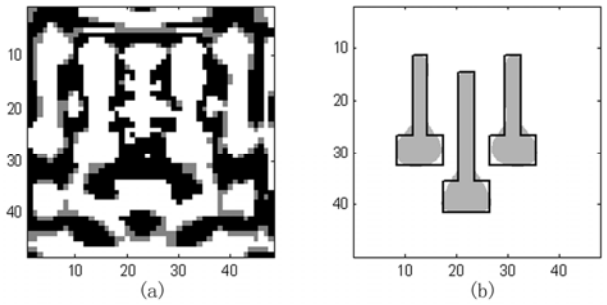

Figure 5. The simulation results for synthesizing APSM: (a) the synthesized APSM mask where black, gray and white pixels have values of -1, 0 and 1, respectively; (b) the corresponding image on wafer.

V. SUMMARY

A novel ILT approach combined with DDL technique for mask synthesis, namely DDL-ILT, is proposed. It addresses the key problem of automatically synthesizing the proper mask patterns for DDL systems. In the flow of the proposed DDL-ILT approach, only one mask is processed to print the wafer image, and this can improves the optimization efficiency.

To evaluate our approach, three variants masks are synthesized for printing 45-nm CD features. The simulation results show that the synthesized masks obtained by DDL-ILT approach can provide excellent fidelity and our approach is capable of synthesizing various kinds of masks.

REFERENCES

[1] B. E. A. Saleh and S. I. Sayegh, "Reduction of errors of microphotographic reproductions by optimal corrections of original masks," Opt. Eng. 20, 781-787(1981).

[2] A. Erdmann, R. Farkas, T. Fuhner, B. Tollkuhn, and G. Kokai, "Towards automatic mask and source optimization for optical lithography," Proc. SPIE 5377, 646-657(2004).

[3] Y. Granik, "Solving inverse problems of optical microlithography," Proc. SPIE 5754, 506-526(2005).

[4] A. Poonawala and P. Milanfar, "OPC and PSM design using inverse lithography: A non-linear optimization approach," Proc. SPIE 6154, 61543H(2006).

[5] P. S. Davids and S. B. Bollepalli, "Generalized Inverse Problem for Partially Coherent Projection Lithography," Proc. SPIE 6924, 69240X (2008).

[6] S. D. Hsu, N. P. Corcoran, M. Eurlings, W. T. Knose, T. L. Laidig, K. E. Wampler, et al., "Dipole Decomposition Mask-design for Full Chip Implementation at the 100nm Technology Node and Beyond," Proc. SPIE 4691, 476-490(2002).

[7] T. B. Chiou, A. C. Chen, S. D. Hsu, M. Eurlings, E. Hendrickx, "Development of automatic OPC treatment and layout decomposition for double dipole lithography for low-k1 imaging," Proc. SPIE 5645, 21-31(2005).

[8] N. Cobb and D. Dudau, "Dense OPC and verification for 45nm," Proc. SPIE 6154, 61540I(2006).

[9] A. Poonawala and P. Milanfar, "Double-exposure mask synthesis using inverse lithography," Journal of Microlithography, Microfabrication and Microsystems, vol. 6, pp. 043001(2007).

[10] M. Born and E. Wolfe, "Principle of Optics," Cambridge University Press (1999).

[11] V. C. Pati and T. Kailath, "Phase-shifting masks for microlithography: Automated design and mask requirements," Journal of Optical Society of America A – Optics Image Science and Vision 9, 2438-2452 (1994).